The EMBO Journal Vol.17 No.24 pp.7190–7198, 1998

Mutations in the pore regions of the yeast K^+ channel YKC1 affect gating by extracellular K^+

Paola Vergani[1], David Hamilton, Simon Jarvis[2] and Michael R.Blatt

Laboratory of Plant Physiology and Biophysics, University of London, Wye College, Wye, Kent TN25 5AH and [2]Research School of Biosciences, University of Kent, Canterbury, Kent CT2 7NJ, UK

[1]Corresponding author
e-mail: p.vergani@wye.ac.uk

The product of the *Saccharomyces cerevisiae* K^+-channel gene *YKC1* includes two pore–loop sequences that are thought to form the hydrophilic lining of the pore. Gating of the channel is promoted by membrane depolarization and is regulated by extracellular K^+ concentration ($[K^+]_o$) both in the yeast and when expressed in *Xenopus* oocytes. Analysis of the wild-type current now shows that: (i) $[K^+]_o$ suppresses a very slowly relaxing component, accelerating activation; (ii) $[K^+]_o$ slows deactivation in a dose-dependent fashion; and (iii) Rb^+, Cs^+ and, to a lesser extent, Na^+ substitute for K^+ in its action on gating. We have identified single residues, L293 and A428, at equivalent positions within the two pore loops that affect the $[K^+]_o$ sensitivity. Substitution of these residues gave channels with reduced sensitivity to $[K^+]_o$ in macroscopic current kinetics and voltage dependence, but had only minor effects on selectivity among alkali cations in gating and on single-channel conductance. In some mutants, activation was slowed sufficiently to confer a sigmoidicity to current rise at low $[K^+]_o$. The results indicate that these residues are involved in $[K^+]_o$ sensing. Their situation close to the permeation pathway points to an interaction between gating and permeation.

Keywords: ion permeation/outward-rectifier K^+ channel/potassium-dependent gating/*Saccharomyces cerevisiae*/site-directed mutagenesis

Introduction

In general, walled cells maintain intracellular homeostasis and transmembrane driving forces in widely differing ionic environments. Such cells have evolved systems capable of sensing and responding to changing ionic gradients across the membrane. The major K^+ outward rectifier of the yeast plasma membrane, encoded by the *YKC1* gene (= *TOK1*, *DUK1* or *YORK*) (Miosga *et al.*, 1994), shows sensitivity to extracellular K^+ concentration ($[K^+]_o$) (Bertl *et al.*, 1993; Ketchum *et al.*, 1995; Lesage *et al.*, 1996; Reid *et al.*, 1996; Vergani *et al.*, 1997). The voltage dependence of gating shifts in parallel with the K^+ electrochemical potential, thus enabling the channel to catalyse effectively only outward K^+ flux. *In vivo*, these characteristics are thought to be important for maintenance of membrane voltage during nutrient uptake, turgor regulation and specialized signalling functions (Bertl *et al.*, 1993; Lesage *et al.*, 1996). In guard cells of higher plants, similar characteristics ensure K^+ efflux for stomatal closure regardless of the external K^+ environment (Blatt and Gradmann, 1997), and analogous dependencies are known in other plant cell types (Blatt, 1991; Thiel and Wolf, 1997). However, the structural determinants of this unusual $[K^+]_o$ sensitivity to gating have yet to be identified in any K^+ channel.

Sequence analysis suggests that YKC1 contains eight transmembrane-spanning domains. The first part of the protein shares structural features with the family of voltage-gated K^+ channels (Kv family) with six transmembrane domains, and a conserved 'pore–loop' (P-loop) sequence linking domains 5 and 6 that is thought to line the K^+-selective permeation pathway. In addition, YKC1 contains a second P-loop inserted between domains 7 and 8. Sequence homology with other K^+ channels is restricted to the two P-loops (Ketchum *et al.*, 1995; Lesage *et al.*, 1996; Reid *et al.*, 1996).

Because K^+ sensitivity is retained in the heterologously expressed *YKC1* gene product (Ketchum *et al.*, 1995; Lesage *et al.*, 1996; Vergani *et al.*, 1997), it is likely that the K^+ sensor is an integral part of the protein structure. In fact, extracellular K^+ has been found to affect animal Kv channel gating (Pardo *et al.*, 1992), albeit in an inactivation gating mechanism known as C-type inactivation (Choi *et al.*, 1991; Liu *et al.*, 1996). At a molecular level, the residue present at position 449 in the *Shaker* pore (two residues C-terminal to the GYGD signature sequence) is known to affect strongly the kinetics of C-type inactivation and its interaction with extracellular K^+ (Lopez-Barneo *et al.*, 1993). These and other results (Baukrowitz and Yellen, 1995, 1996; Ranganathan *et al.*, 1996) have suggested the existence of a K^+-binding site near the outer mouth of the pore which, when occupied, would slow C-type inactivation.

We suspected that the $[K^+]_o$-sensing function of the P-loop of Kv channels might have been retained in the YKC1 channel but coupled to different gating transitions. In YKC1, a leucine in the first P-loop and an alanine residue in the second P-loop are found in the position corresponding to *Shaker* T449. We altered these residues by site-directed mutagenesis and examined the functional effects of these changes after heterologous expression in *Xenopus laevis* oocytes. Here we report that extracellular K^+ affects the kinetics of activation and deactivation as well as the voltage dependence of gating of the wild-type channel. Substitutions in the second P-loop, and to a lesser extent in the first P-loop, alter these kinetic and steady-state characteristics by reducing the channel sensitivity to $[K^+]_o$.

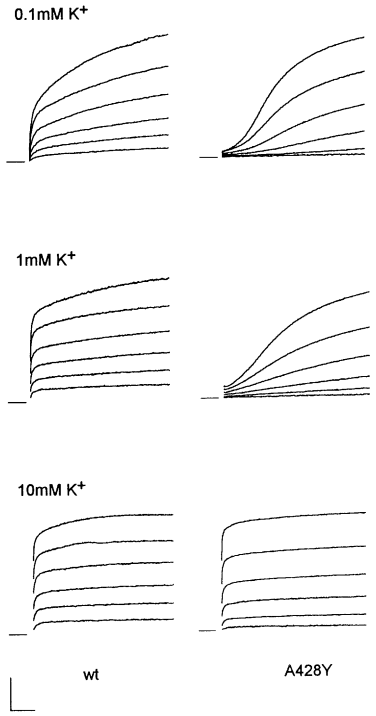

Fig. 1. Extended clamp steps uncover an additional, very slow-activating component to YKC1 activation that is suppressed by extracellular K^+ and augmented by mutation. $[K^+]_o$ dependence of current activation kinetics for wild-type (left column) and the A428Y mutant (right column) YCK1 currents expressed in oocytes. Families of current trajectories recorded upon stepping to voltages between –30 mV and +70 mV, following a 10 s conditioning step to –120 mV. External K^+ concentration is as indicated. The zero current level is indicated by each set of traces (left). Scale: vertical, 10 μA; horizontal, 5 s.

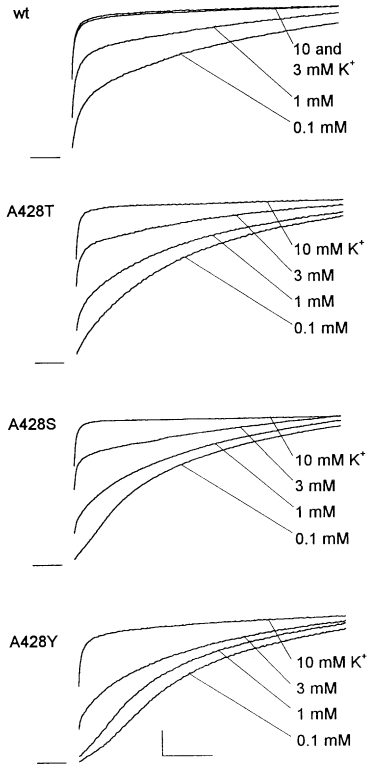

Fig. 2. Amino acid substitutions at residue A428 effect a slowing of YKC1 current activation that can be overcome by raising external K^+ concentration. Current trajectories from wild-type and from A428T, A428S and A428Y YKC1 mutant channels normalized to estimated current maxima (I_{max}; Figure 4). Data were recorded upon voltage steps to +50 mV at 0.1, 1, 3 and 10 mM $[K^+]_o$ following 10 s conditioning steps to –120 mV. Scale: vertical, 0.2 relative units; horizontal, 5 s.

Results

Identification of a very slow, K^+-dependent component of wild-type YKC1 activation

Previous analyses of macroscopic ionic currents carried by the wild-type YKC1 channel had distinguished two kinetically distinct components: part of the current appeared within 1–2 ms after depolarization (the 'instantaneous' component) while the rest activated more slowly with a time constant of ~1 s (Lesage *et al.*, 1996; Loukin *et al.*, 1997; Vergani *et al.*, 1997), hereafter designated as the 'fast' component. In the present study, we observed that if the duration of the depolarization was increased to tens of seconds, an additional, much slower kinetic component could be discerned which we will refer to as the slow component. Figure 1 (left) shows whole-cell currents recorded in YKC1-expressing *Xenopus* oocytes in response to 30 s steps to increasingly depolarized voltages. This slow component was strongly dependent on $[K^+]_o$, being most evident at sub- and low millimolar $[K^+]_o$ conditions (0.1 mM, top left) under which it comprised a significant fraction of the total current.

The effects of $[K^+]_o$ on the distribution of total current among the different kinetic components is illustrated in Figure 2 (top). The panel shows current traces evoked by voltage steps to +50 mV at the indicated $[K^+]_o$, normalized to the estimated steady-state current. The slowest activation was recorded with 0.1 mM $[K^+]_o$, and the rate of current rise progressively increased as $[K^+]_o$ was raised to 1, 3 and 10 mM. The time course for the activation of the wild-type current could be well described as the sum of a constant term plus two exponentials corresponding to the instantaneous, fast and slow components, respectively. Parameters obtained from the fittings (see below) showed that the major effect of increasing $[K^+]_o$ was to decrease the relative amplitude of the slow component. Thus, increasing $[K^+]_o$ accelerated the overall time course of activation by favouring the other, faster, components.

Mutations in the pore enhance slow activation

We found that substituting the alanine at position 428 in the second P-loop with a tyrosine had a dramatic effect on the kinetics of activation at low $[K^+]_o$. Figure 1 (right) shows families of relaxation curves in oocytes expressing the A428Y mutant YKC1 channel. At 0.1 mM $[K^+]_o$, the current showed little instantaneous component and rose with a slow, distinctly sigmoidal time course (Figure 1, top right). Again, increasing $[K^+]_o$ accelerated the overall activation and, in addition, progressively reduced the sigmoidal character so that in 10 mM $[K^+]_o$ (Figure 1, bottom right), wild-type and A428Y current relaxations were virtually indistinguishable. The accelerating effect of $[K^+]_o$ for the A428Y mutant is also shown in the last panel of Figure 2, where the normalized currents measured at increasing $[K^+]_o$ are superimposed.

Patch-electrode recordings from oocytes expressing wild-type and A428Y mutant channels indicated that the

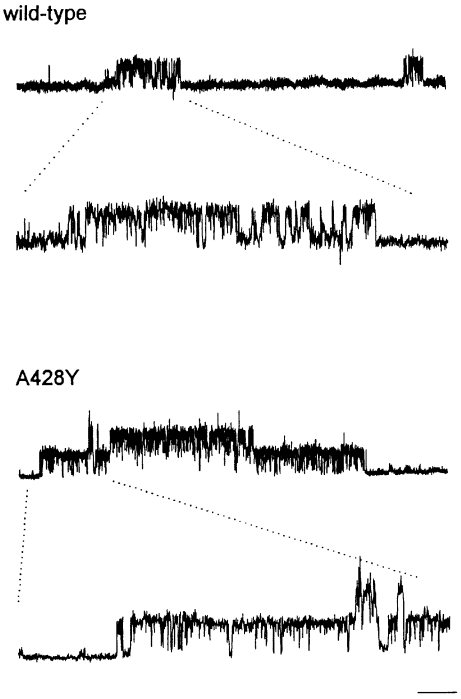

Fig. 3. Single-channel current amplitude of YKC1 is not affected by the A428Y mutation. Current from cell-attached patches in oocytes expressing wild-type (top) and the A428Y mutant (bottom) YKC1 channel recorded at a pipette voltage of –120 mV (≅ +50 mV membrane voltage = cell voltage – pipette voltage; nominal cell voltage, –70 mV). Bath and pipette solutions both contained 1 mM K^+. Time scale: 1 s or 200 ms for the expanded traces.

mutation did not have an appreciable effect on the single-channel properties. In oocytes expressing the wild-type channel, cell-attached and isolated patch measurements showed the characteristic flickery bursts of YKC1 (Figure 3,wild-type, Cs^+ and Rb^+ were roughly equivalent and more effective than K^+ top), and estimates of single-channel conductance gave values of 25 ± 4 pS, comparable to previous reports (Bertl *et al.*, 1993; Zhou *et al.*, 1995; Lesage *et al.*, 1996). Similar current characteristics were observed in oocytes expressing the A428Y mutant (Figure 3, bottom), and estimates of single-channel conductance for the A428Y mutant gave a value of 23 ± 3 pS. We were unable to identify any obvious differences in single-channel kinetics within recording periods of 30–100 s (data not shown). However, because mutation might be expected to affect the very slowest components of closed time distributions (see Discussion), our recordings probably contained an insufficient number of events to obtain reliable estimates for these.

To gain an insight into possible links between the physico-chemical characteristics of residues at position 428 and their functional effects, other amino acids were substituted for the alanine. The presence of threonine or serine at this position resulted in a qualitatively similar, albeit less severe slowing of activation kinetics (Figure 2, central panels). Substitutions with lysine, aspartic acid, phenylalanine and leucine failed to give functional channels. Mutants at the homologous residue in the first P-loop, L293, were also examined. In this case, the L293Y mutant displayed activation kinetics virtually indistinguishable from wild-type. However, the L293S and L293A mutants

Table I. Fitted parameter values for Figure 4 (insets)

	$[K^+]_o$ (mM)	a_i	a_f	a_s	k_f (s^{-1})
Wild-type	0.1	0.03	0.35	0.62	1.13
	1.0	0.19	0.48	0.34	1.77
	3.0	0.45	0.46	0.10	1.99
	10.0	0.42	0.50	0.08	2.17
A428Y	0.1	0.03	–0.44	1.41	0.15
	1.0	0.10	–0.11	1.01	0.44
	3.0	0.35	0.03	0.62	0.49
	10.0	0.56	0.30	0.14	1.38

exhibited slower activation with sigmoidal kinetics in 0.1 mM $[K^+]_o$ (data not shown), similar to the A428S mutant. To explore possible interactions between mutations at residues A428 and L293, we constructed double mutants. Currents carried by the L293Y–A428Y double mutant were found not to differ measurably from A428Y currents (data not shown), and oocytes injected with cRNA encoding the L293S–A428S double mutant failed to express functional channels.

Mutations reduce the sensitivity of activation to $[K^+]_o$

Overall, mutations at residues 428 and, to a lesser extent, 293 affected activation kinetics so that at any one $[K^+]_o$, activation of the mutant was slowed by comparison with the wild-type. In each case, this effect of the mutation could be overcome by increasing $[K^+]_o$ as in the wild-type, although higher concentrations of K^+ were required. Thus, the effect of mutation was to reduce the sensitivity of the channel gate to $[K^+]_o$, as can be appreciated qualitatively by comparing the trajectories in Figure 2 (compare wild-type in 0.1 mM $[K^+]_o$ with A428T and A428S in 1 mM $[K^+]_o$ and A428Y in 3 mM $[K^+]_o$).

A quantitative analysis of the reduction in $[K^+]_o$ sensitivity in the mutants is shown in Figure 4. Current relaxations for the mutants were well described by equation 1, containing a constant term and two exponential components, as was the case for the wild-type (see Figure 4A, insets). To a first approximation, $[K^+]_o$ accelerated the overall rate of current increase by displacing the current kinetics between the slow and the other kinetic components. We therefore used the amplitudes of the time-dependent components obtained from fittings to construct dose–response curves (Figure 4A). For both wild-type and mutant channels, the relative amplitude of the fast component $[a_f/(a_f + a_s)]$ rose with $[K^+]_o$ in a dose-dependent fashion. The data were well fitted to the Hill equation (equation 2) and, in joint fittings of the means, yielded a common cooperativity coefficient near 2 (Figure 4A, solid lines). In each case, mutation in the second P-loop lowered the apparent affinity for $[K^+]_o$. The A428Y mutant was the most dramatically affected, while substitution of the alanine with threonine had a smaller effect [means ± SE (*n*): wild-type, $K_{1/2}$ = 1.3 ± 0.2 mM (4); A428Y, $K_{1/2}$ = 3.9 ± 0.3 mM (4); A428T, $K_{1/2}$ = 3 ± 0.3 (3)]. By contrast, the L293Y and L293S substitution in the first P-loop resulted in a $K_{1/2}$ that did not differ significantly from the wild-type, while a small increase in $K_{1/2}$ was observed when alanine was substituted for the leucine [mean ± SE (*n*): L293Y, $K_{1/2}$ = 0.8 ± 0.2 (4);

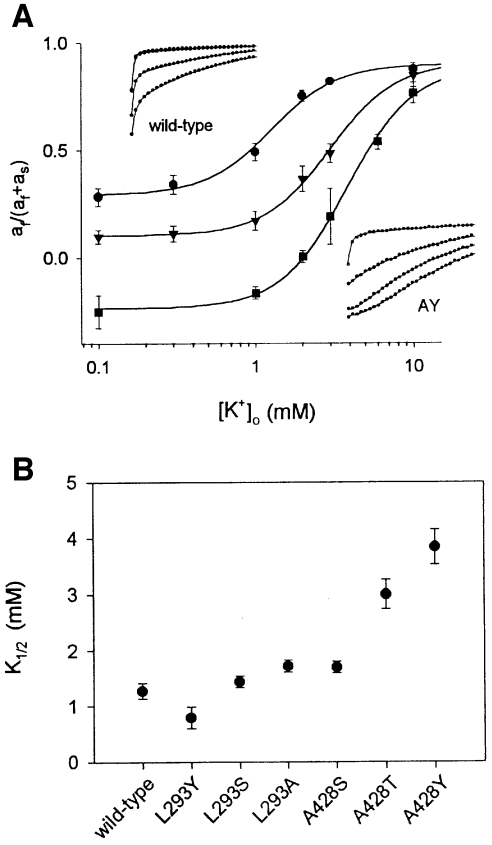

Fig. 4. Mutations reduce the sensitivity of YKC1 current activation to extracellular K^+. (**A**) Amplitude of the fast component, relative to the total amplitude of the time-dependent components [$a_f/(a_f + a_s)$], plotted as a function of $[K^+]_o$. Amplitudes were determined by fitting sets of current relaxations (see Figure 2) to a double exponential equation of the form

$$I/I_{max} = a_i + a_f(1 - e^{-k_f t}) + a_s(1 - e^{-k_s t}) \quad (1)$$

with k_s held in common. Here a_i, a_f and a_s are the relative amplitudes of the instantaneous, fast and slow components, k_f and k_s are the corresponding rate constants, and I_{max} is the predicted maximum steady-state current. Data (means ± SE) were obtained from oocytes expressing wild-type (●, four cells), A428T (▼, three cells) and A428Y (■, four cells) YKC1 channels. Curves are the results of fittings to the Hill equation:

$$y = y_0 + y_{max}\frac{[K^+]^n}{K_{1/2}^n + [K^+]^n} \quad (2)$$

Best fittings (solid lines) were obtained with the Hill coefficient held in common between data sets, including data from A428S, L293S, L293A and L293S mutants (not shown), and gave a value of $n = 2.1 \pm 0.3$. Fitted values: y_0: wild-type, 0.29 ± 0.02; A428T, 0.1 ± 0.03; A428Y, –0.24 ± 0.02; y_{max}: wild-type, 0.61 ± 0.03; A428T, 0.8 ± 0.04; A428Y, 1.1 ± 0.06; values for $K_{1/2}$ are given in the text. Insets: current relaxations of two sample data sets, wild-type and A428Y, showing the results of fittings (solid lines) to equation 1. For clarity, only every one-hundredth data point is shown. Fitted parameter values are shown in Table II. Values for k_s were held in common between relaxations within each set. For the sets shown, k_s values in each case were 0.05/s. Note that the sigmoidicity of the activation kinetics in the A428Y mutant implies a negative value for a_f in the solution to equation 1 and, hence, values less than zero in the ratio $a_f/(a_f + a_s)$ at low $[K^+]_o$. (**B**) Scatter plot showing means ± SE of $K_{1/2}$ values obtained from analyses as in (A) for the different mutants. At least three cells were analysed for each mutant.

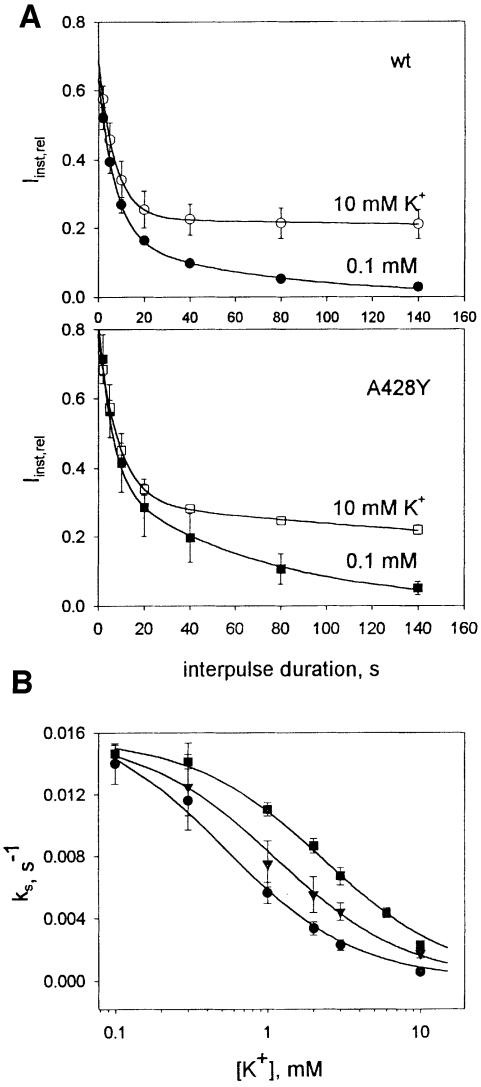

Fig. 5. Mutations reduce the sensitivity of YKC1 current deactivation to extracellular K^+. Transit into distal closed states measured as the rate of escape from instantaneous reactivation in three-step protocols. (**A**) Fraction of instantaneously activatable current ($I_{inst,rel}$) as a function of time at –120 mV (interpulse duration). Voltage clamp protocol: 30 s conditioning (activating) step to +50 mV; interpulse step to –120 mV of variable duration; and 200 ms test pulse to +50 mV. $I_{inst,rel}$ measured at 10 ms from the start of the test pulse, normalized to the current value measured at the end of the 30 s activating step and plotted as a function of interpulse duration. Data are shown for wild-type (top) and A428Y mutant (bottom) channels in 0.1 mM (●, ■) and 10 mM (○, □) $[K^+]_o$. Curves represent fittings to a double exponential equation of the form:

$$I_{inst,rel} = a_{df}e^{-k_f t} + a_{ds}e^{-k_s t} \quad (3)$$

where a_{df} and a_{ds} are the relative amplitudes of the fast and slow components, and k_f and k_s are the corresponding rate constants. (**B**) Effect of $[K^+]_o$ on the k_s parameter obtained from the analysis shown in (A). Rate constants (means ± SE) obtained for wild-type (●, five cells), A428T (▼, four cells) and A428Y (■, five cells) are plotted. Solid lines are the results of fittings to a logistic function of the form:

$$k_s = \frac{R}{1 + \dfrac{[K^+]_o}{K_{1/2}}} \quad (4)$$

where $K_{1/2}$ is the $[K^+]_o$ at which k_s has dropped to half of the maximal value R. Fitted parameters: $R = 0.017 \pm 0.001$ for wild-type and 0.016 ± 0.001 for both mutants; $K_{1/2}$ values are given in the text.

L293S, $K_{1/2}$ = 1.4 ± 0.1 (3); L293A, $K_{1/2}$ = 1.7 ± 0.1 (3)]. Results obtained from each of the mutant channels are summarized in Figure 4B.

Mutations reduce the sensitivity of deactivation to $[K^+]_o$

To investigate the effect of $[K^+]_o$ on deactivation upon repolarization, we used a two-pulse protocol varying the interpulse intervals. The current was activated with 30 s steps to +50 mV and the voltage then stepped to –120 mV for varying lengths of time. The channel population remaining in the instantaneously activatable pool at the end of this period was then assayed 10 ms into a second step to +50 mV and the current normalized to the steady-state current recorded at the end of the first, 30 s step. The curves in Figure 5A show the fraction of current reactivated 'instantaneously' as a function of the –120 mV interpulse duration and indicate the time course of relaxation into more distal closed states from which only time-dependent reactivation was possible.

At every $[K^+]_o$, the instantaneously reactivated current decreased, even over periods as long as 140 s, consistent with its decay to vanishingly small values when hyperpolarization was maintained for sufficiently long times. Each curve was well described by the sum of two falling exponentials (equation 3; Figure 5A). The rate constant of the slowest component declined as $[K^+]_o$ was increased in every case, while the rate constant for the other component was largely independent of $[K^+]_o$ in the wild-type and exhibited limited sensitivity below 1 mM $[K^+]_o$ in A428Y and A428T (not shown). Concentrations giving half-maximal reduction in the rate constant for the slowest component were estimated by fitting to a logistic (dose–response) function (equation 4; Figure 5B). As was observed for acceleration of activation, mutations decreased the apparent affinity for $[K^+]_o$ [mean ± SE (*n*): wild-type, $K_{1/2}$ = 0.5 ± 0.1 (5); A428T, $K_{1/2}$ = 1.1 ± 0.2 (4); A428Y, $K_{1/2}$ = 2.3 ± 0.2 (5)]. Thus $[K^+]_o$ appeared to slow the rate of transitions out of the open state into the more distal closed states of the channel, and mutations at residue 428 shifted the dose–response curves to higher K^+ concentrations.

Mutations reduce the $[K^+]_o$ sensitivity of the steady-state voltage dependence

We found that mutation at residue 428 also affected the steady-state characteristics of YKC1 current. Figure 6 shows the voltage dependence of steady-state activation, for wild-type and the A428Y mutants. Current–voltage (I–V) curves for the wild-type showed the characteristic outward rectification of YKC1 and shift towards more positive potentials as $[K^+]_o$ was increased from 10 mM to 30 and 100 mM. However, as we had previously observed (Vergani *et al.*, 1997), the magnitude of this shift was not Nerstian but decreased in the low millimolar $[K^+]_o$ range, with a threshold near 1 mM $[K^+]_o$, below which no further $[K^+]_o$ dependence was measurable. For A428Y (Figure 6, insets) and A428T mutants (data not shown), this threshold was raised above 10 mM $[K^+]_o$. By contrast, the slope of the voltage dependence for channel opening as determined by the Boltzmann voltage sensitivity coefficient, δ (equation 5; Figure 6), was insensitive to $[K^+]_o$ and unaffected in the mutants. Thus, these mutations resulted in a displacement of the $[K^+]_o$ sensitivity of the YKC1 I–V relationship to higher K^+ concentrations without altering the inherent voltage sensitivity of the macroscopic conductance itself.

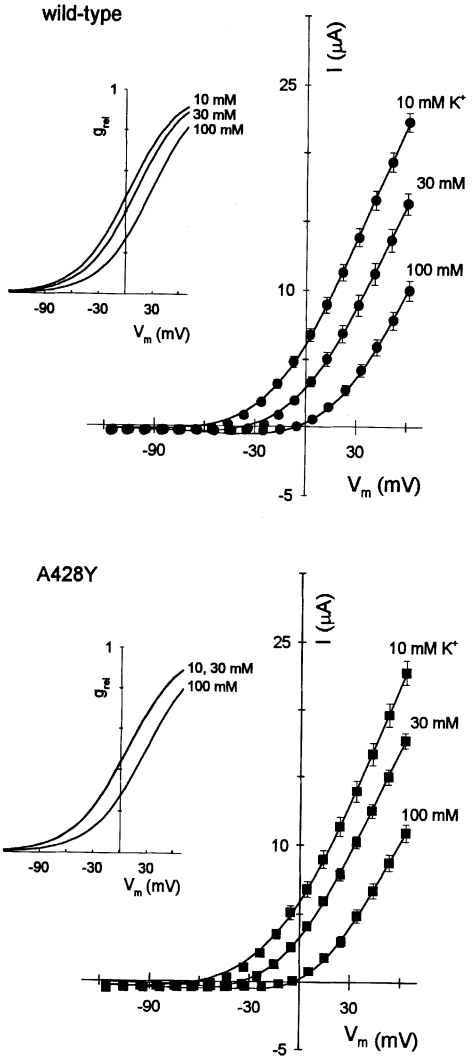

Fig. 6. Mutations reduce the $[K^+]_o$ sensitivity of steady-state voltage dependence for opening. Current–voltage relationships for wild-type (top) and the A428Y mutant (bottom) YKC1 measured in 10, 30 and 100 mM $[K^+]_o$ as indicated, fitted jointly to a Boltzmann function (solid lines) of the form:

$$I = \frac{g_{\max}\,(V - E_K)}{1 + e^{\delta F(V - V_{1/2})/RT}} \qquad (5)$$

where I is the current at voltage V, $g_{\max}$ is the maximum steady-state conductance, δ is the voltage sensitivity coefficient (= apparent gating charge), $V_{1/2}$ is the voltage at which the steady-state conductance $g = g_{\max}/2$, and F, R and T have their usual meanings. Because the current reversal potential could not be obtained directly from tail current analyses, the K^+ equilibrium voltage, E_K, was defined from the Nernst equation and fittings carried out jointly holding the parameter for the intracellular $[K^+]$ in common. Steady-state currents recorded at the end of 5 s steps (see Figure 1). Insets: corresponding relative conductance (g_{rel})–voltage curves derived from the fitted current–voltage curves. Fitted parameters (mean ± SE): wild-type (seven cells): δ, 0.9 ± 0.1, $V_{1/2}$, 3 ± 2 mV (10 mM), 12 ± 2 mV (30 mM), 29 ± 4 mV (100 mM $[K^+]_o$); $[K^+]_i$, 129 ± 5 mM; A428Y (seven cells): δ, 0.9 ± 0.2, $V_{1/2}$, 8 ± 2 mV (10 mM), 8 ± 2 mV (30 mM), 29 ± 4 mV (100 mM $[K^+]_o$); $[K^+]_i$, 130 ± 6 mM.

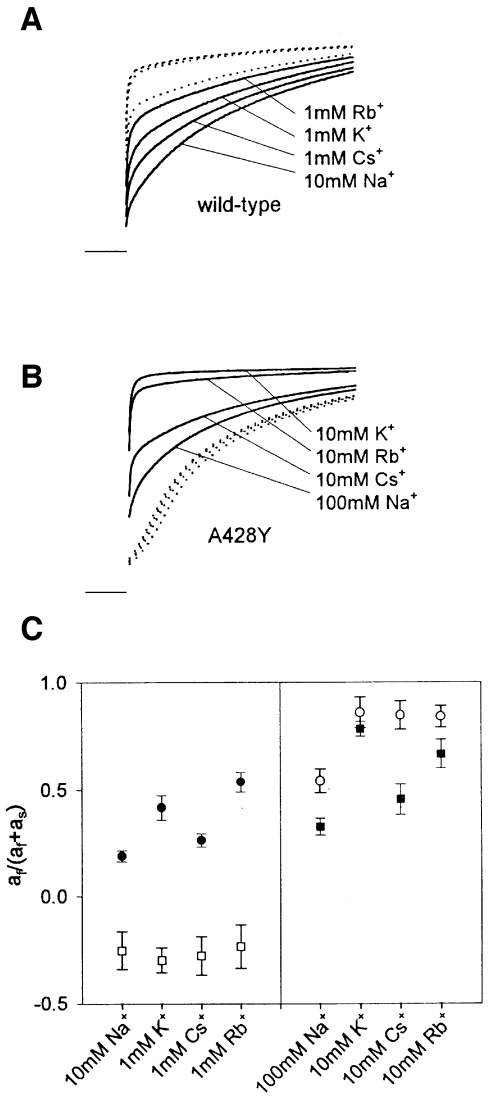

Fig. 7. Alkali cations substitute for K^+ in accelerating activation kinetics. (**A**) Wild-type and (**B**) A428Y mutant current relaxation traces obtained during voltage steps to +50 mV (see Figure 2) with the indicated concentrations of K^+, Rb^+, Cs^+ and Na^+ present in the bathing solution. The total monovalent cation concentration was kept constant at 100 mM by substitutions with NMG. Traces measured in 10 mM alkali cation concentrations (or 100 mM Na^+) for the wild-type, and in 1 mM alkali cation concentrations (or 10 mM Na^+) for the A428Y are shown as dotted lines. (**C**) The relative amplitude of the fast-relaxing component, $a_f/(a_f + a_s)$ derived from fittings to equation 1 (see Figure 4), plotted for the alkali cations and concentrations indicated below. Data are means ± SE (wild-type: ● ○, four cells; A428Y, ■ □, seven cells). Open symbols correspond to dotted traces in (A) and (B).

Other monovalent cations affect kinetics and voltage dependence of gating

We tested the specificity for K^+ in controlling YKC1 activation kinetics and the voltage sensitivity of the steady-state current by substituting extracellular K^+ with Rb^+, Cs^+ and Na^+ while maintaining the total cation concentration constant with *N*-methylglucamine (NMG). As illustrated in Figure 7A and B, $[Rb^+]_o$, $[Cs^+]_o$ and, to a much lesser extent, $[Na^+]_o$ were effective in accelerating activation kinetics of the YKC1 current. For the wild-type, this effect was seen most clearly at low millimolar cation concentrations, whereas at higher concentrations, at which the effect of $[K^+]_o$ on the relative amplitude of the fast component saturated (Figure 4A), the difference in actions of K^+, Rb^+, Cs^+ and, to a certain extent, of Na^+ on current activation was largely masked (Figure 7A, dotted lines). A similar dependence was evident for the A428Y mutant current (Figure 7B). However, 10-fold higher concentrations of each cation were required to evidence differences in efficacy, consistent with the shift in the mutant dose–response curve for $[K^+]_o$ (Figure 4A). Little difference in the current kinetics was observed at 1 mM concentrations of K^+, Rb^+ and Cs^+, and with 10 mM Na^+ (Figure 7B, dotted lines).

Table II. Alkali cations substitute for K^+ in modulating the voltage sensitivity of gating

		Wild-type	A428Y
$V_{1/2}$ ± SE (mV)	10 mM K^+	3.2 ± 1.5	7.7 ± 1.8
	10 mM Rb^+	12.1 ± 1.3	20.8 ± 1.2
	10 mM Cs^+	7.3 ± 1.3	39.4 ± 0.2

Values for $V_{1/2}$ determined from fittings of current–voltage curves (see Figure 6) to Equation (5) on the assumption of equal permeability between the cations K^+,Cs^+ and Rb^+. Assuming a 10:1 permeability ratio for K^+:Cs^+ and K^+:Rb^+ gave the same ordering of efficacies in displacement of $V_{1/2}$, but with values for Rb^+ and Cs^+ shifted further positive relative to K^+.

As before, we quantified the potency of the cations on current relaxations using the relative amplitude of the fast component $[a_f/(a_f + a_s)]$ obtained by fitting sets of data to equation 1 (Figure 4), including those shown in Figure 7A and B. Extracellular K^+ and Rb^+ were found not to have significantly different potencies, while Cs^+ was slightly less effective for both the A428Y mutant and wild-type YKC1 currents. Extracellular Na^+ also accelerated channel activation kinetics, but the effect was visible only at much higher concentrations: 100 mM Na^+ gave rates comparable with those measured in the 1–10 mM concentration range for Rb^+, Cs^+ and K^+ (Figure 7A, B and C). Thus, the potency of cations in acceleration of YKC1 activation followed the series: $Rb^+ \approx K^+ > Cs^+ \gg Na^+$.

Previous studies had also shown that Rb^+ and Cs^+ affect the voltage sensitivity of the wild-type YKC1 current in the steady-state (Vergani *et al.*, 1997). We compared the voltage sensitivities of the wild-type and A428Y mutant currents, extracting the voltage for half-maximal activation, $V_{1/2}$, from steady-state current–voltage data as in Figure 6, but recorded in 10 mM K^+, Rb^+ and Cs^+. Table II summarizes results from 13 cells and shows that Rb^+ and Cs^+ were slightly more effective than K^+ in displacing the voltage dependence of the wild-type current towards more positive values. For the A428Y mutant, the results yielded a potency sequence $Cs^+ > Rb^+ > K^+$.

Discussion

The outward rectifier YKC1 mediates K^+ efflux in yeast and when expressed in *Xenopus* oocytes. While the K^+ ions carrying the current derive from the intracellular pool, gating of the channel, like that of many K^+ channels in plants (Blatt, 1991; Blatt and Gradmann, 1997; Thiel and Wolf, 1997), is modulated by extracellular K^+. Our study now identifies key aspects of the molecular mechan-

ism underlying gating modulation by $[K^+]_o$: (i) we have uncovered the existence of a very slow component of current activation, the relative magnitude of which is strongly favoured by low $[K^+]_o$; (ii) we find that single point mutations at a residue located at the outer mouth of the pore within the second P-loop cause a dramatic slowing of activation kinetics, faster deactivation and a reduced $[K^+]_o$ sensitivity of the steady-state voltage dependence, effects that can be overcome with a sufficient increase in $[K^+]_o$; (iii) mutations at the homologous position in the first P-loop result in qualitatively similar but less severe phenotypes; and (iv) we have observed that gating of the current shows a selectivity among alkali cations which is largely retained on mutation. The reduced sensitivity towards $[K^+]_o$ shown by our mutants strongly suggests that the regulatory binding site(s) for extracellular K^+ are close to the mutagenized residues, in the outer mouth of the pore. Furthermore, our results indicate that the two pore domains are not functionally equivalent.

Our observation of the slowest component to current activation can be accommodated within the context of the serial state model proposed before (Lesage *et al.*, 1996; Loukin *et al.*, 1997; Vergani *et al.*, 1997), and comparable with a similar model for the K^+ channels of stomatal guard cells (Blatt and Gradmann, 1997), by introducing a further distal closed state (C_4) connected to the others by a very slow transition (rate constants k_{43} and k_{34}):

$$C_4 \underset{k_{43}}{\overset{k_{34}}{\rightleftharpoons}} C_3 \underset{k_{32}}{\overset{k_{23}}{\rightleftharpoons}} C_2 \underset{k_{21}}{\overset{k_{12}}{\rightleftharpoons}} O_1 \qquad \text{(S1)}$$

According to this model, the channel must pass sequentially through up to three closed states (C_4, C_3 and C_2) before reaching the open state (O_1). Negative voltage favours channel residence in the distal closed states while depolarization favours transit to the open state. Transit between C_2 and O_1 is virtually instantaneous (Lesage *et al.*, 1996; Vergani *et al.*, 1997) while fast activation (τ ~1 s) had been associated with transit out of the more distal closed state C_3. It is clear that transit between C_4 and C_3 must be appreciably slower still for the slowest component to appear in the current trajectories (Figures 1 and 2). Thus, the relative occupancy of each of these states immediately preceding a positive voltage step determines the relative amplitude of the instantaneous, fast and slow components to current activation.

Extracellular K^+ affects YKC1 gating in two opposing ways. We previously had shown (Vergani *et al.*, 1997) that $[K^+]_o$ >1–3 mM alters the distribution between the instantaneous and time-dependent components of the current, favouring the latter. This observation, and the shift of the steady-state conductance–voltage relationship to more positive voltages with increasing $[K^+]_o$, indicated that K^+ binding tends to draw channels out of the open state and toward the C_3 state. In contrast, in the present studies, we found that high $[K^+]_o$ accelerated channel activation, reducing the relative contribution of the slow component to current activation (Figures 1, 2 and 4). Increasing $[K^+]_o$ also delayed exit from the instantaneously activatable pool by reducing the slower of the two relaxation rate constants in channel deactivation (Figure 5). These observations suggest that at high $[K^+]_o$ a larger proportion of channels populate closed states near the open state.

This dual effect can be accounted for if the two separate transitions, $C_4 \rightleftharpoons C_3$ and $C_3 \rightleftharpoons C_2$, are affected in opposing fashion by $[K^+]_o$ so that increasing $[K^+]_o$ stabilizes the conformation corresponding to the C_3 state and draws channels out of the adjacent states, whether C_4 or C_2 (i.e. k_{43} and k_{23} are pseudo-first-order rate constants describing the K^+-binding steps). The fact that these effects are mediated by $[K^+]_o$ over two distinct concentration ranges suggests an action of K^+ at two regulatory binding sites with differing affinities. Thus, in low $[K^+]_o$, when occupancy of C_4 is favoured over the C_3 state, depolarization leads to activation dominated by the slow $C_4 \rightleftharpoons C_3$ transition. In higher $[K^+]_o$, as the first of the two sites is bound, occupancy of the C_3 state is favoured over C_4, and the $C_3 \rightleftharpoons C_2$ transition comes to dominate current activation. Finally, as K^+ binds to the low affinity site at still higher $[K^+]_o$, the C_3 state is stabilized relative to C_2 and O_1, and a stronger depolarization is required to drive channels into the open state.

Analyses of the site-directed mutants support this interpretation and identify molecular structures that contribute to $[K^+]_o$ sensing of the YKC1 gate. We found that substitutions at A428 near the C-terminus of the second P-loop—and its counterpart L293 in the first P-loop—enhanced the slow component of activation (Figures 1 and 2) and accelerated the slower of the two relaxation components in channel deactivation (Figure 5) without significantly affecting the single-channel current (Figure 3). The effect of the mutations can be interpreted as altering the relative occupancy among the closed states, but in this case in a manner directly opposing the effects of $[K^+]_o$. Dose–response relationships for $[K^+]_o$ action on current activation (Figure 4) and deactivation (Figure 5) showed that the apparent affinity for K^+ was reduced marginally in the first P-loop mutants L293S and L293A, and markedly in the second P-loop mutants A428T and especially A428Y. Thus, the residues A428 and L293 are likely to form part of the regulatory K^+-binding site(s) or to affect accessibility. However, we cannot exclude that the mutations may affect the coupling of K^+ binding to protein conformational changes required for gating.

The fact that the A428Y mutation in the second P-loop had little effect on the alkali cation selectivity for current activation (Figure 7), but did alter the relative potencies of Rb^+ and Cs^+ in displacing its steady-state voltage sensitivity, again suggests the presence of two separate binding sites with distinct actions. The kinetics of current activation, itself, showed an apparent 2-fold cooperativity in its sensitivity to $[K^+]_o$ in both the wild-type and mutant channels (Figure 4A). The observation is interpreted most easily if the cooperative binding of two K^+ ions is required for this kinetic response alone, and would be consistent with the 2-fold symmetry of a channel with four P-loops but comprised of two homologous monomers (MacKinnon, 1995; Goldstein, 1996). Alternatively, the apparent cooperativity might be understood, even in the absence of cooperative K^+ binding, if the response to ligand binding comprised a feed-forward process (Goldbeter and Koshland, 1981; Koshland *et al.*, 1982).

For the second P-loop, the severity of the mutation appeared to be related to the size of the residue. However,

steric hindrance is certainly not the only factor involved. In the first P-loop, the L293S mutant showed kinetic characteristics comparable with those of the A428S mutant, but the L293Y mutant was indistinguishable from the wild-type channel whereas the A428Y mutant was the most severely affected of all the expressing forms. The lack of parallel effect between these two sets of mutants clearly distinguishes the two P-loop domains and suggests that they do not contribute equally to the structure of the channel. It is notable, too, that mutants in the second P-loop that gave rise to functional channels all contained a hydroxyl group. Hydroxyl residues will interact with cations in solution by substituting for water molecules of the hydration shell (Creighton, 1993), so it is possible to envisage that these mutants introduce secondary energy wells that affect access to or interaction with the physiological binding site.

We noted initially that the positions of residues A428 and L293 within the P-loops correspond to T449 of the *Shaker* K^+ channel. In the *Drosophila* and related animal Kv channels, mutations at this site are known to affect C-type inactivation and its sensitivity to extracellular K^+ (Lopez-Barneo *et al.*, 1993; Baukrowitz and Yellen, 1995; Schlief *et al.*, 1996). Protein conformational events in C-type inactivation and in YKC1 gating are not localized only to the outer mouth of the pore, but appear to be influenced by protein domains that lie on the cytosolic side of the membrane (Baukrowitz and Yellen, 1995, 1996; Ogielska *et al.*, 1995; Loukin *et al.*, 1997; Wang *et al.*, 1997). Furthermore, both processes are characterized by very slow kinetics with time constants of several seconds. These parallels suggest that similar structural rearrangements (Yellen *et al.*, 1994; Liu *et al.*, 1996), perhaps with common evolutionary origins, may occur in Kv channel inactivation and in YKC1 activation.

Based on sequence homologies to the *Streptomyces* KcsA K^+ channel, the A428 and L293 residues in YKC1, like T449 of *Shaker*, probably protrude into the outer vestibule of the pore and are situated immediately outside the entry to the K^+ selectivity filter (Doyle *et al.*, 1998). Residues at this position could affect access to the binding sites within the selectivity filter. It is possible, therefore, that the K^+ sensitivity of the gate may depend on K^+ binding within the K^+ selectivity filter itself (Baukrowitz and Yellen, 1996; Kiss and Korn, 1998). In this respect, future studies comparing the selectivity of permeation with the efficacy of action on gating of alkali cations will be informative.

In conclusion, the molecular determinants of permeation and K^+-dependent gating both appear to reside within the pore region. A similar picture has emerged for cyclic nucleotide-gated channels in which the pore region forms a selectivity filter and functions as a channel gate (Sun *et al.*, 1996). Because, on one hand, K^+ binding to the site(s) within or near to the diffusion pathway affects transition rates, changing the open probability of the YKC1 channel, and, on the other hand, outward K^+ flux through the open channel probably raises the local concentration of K^+ at the site, it can be expected that permeation and gating are strongly interlinked processes (Richard and Miller, 1990; Baukrowitz and Yellen, 1995; Chapman *et al.*, 1997; Schneggenburger and Ascher, 1997).

Materials and methods

Molecular biology

The pEXTM1 plasmid (Vergani *et al*., 1997), containing the YKC1open reading frame inserted between the 3′- and 5′-untranslated sequences of the the *Xenopus* β-globin gene of the expression vector pBSXG1 (Groves and Tanner, 1992), was used for mutagenesis, wild-type and mutant YKC1 channel expression. Mutagenesis was carried out by 'long primer' modification of the unique site elimination strategy (Ray and Nickoloff, 1992) using a USE Mutagenesis kit (Pharmacia). Double mutant constructs were generated by inserting the *Bst*XI fragment containing a mutation in the second P-loop into plasmids previously mutagenized in the first P-loop. The accuracy of mutagenesis was checked in every case by sequencing on an ABI Prism310 DNA sequencer. Plasmids were linearized by digestion with *Hin*dIII, and G(5′)ppp(5′)G-capped cRNA was synthesized using T7 polymerase (Cap-Scribe kit, Boehringer Mannheim).

Electrophysiology

Stage V and VI oocytes were taken from mature *Xenopus laevis* and maintained at 18°C in a modified Barth's medium containing 88 mM NaCl, 1 mM KCl, 0.33 mM $Ca(NO_3)_2$, 0.41 mM $CaCl_2$, 0.82 $MgSO_4$, 2.4 mM Na_2CO_3, 0.1 mg/ml gentamycin sulfate and 80 U/ml penicillin. Oocytes were defolliculated manually using fire-polished Pasteur pipettes after partial digestion of the follicular cell layer by incubation for 1 h in modified Barth's medium with 2 mg/ml collagenase supplemented with 1 mg/ml of trypsin inhibitor (Sigma). Defolliculated oocytes were injected with 5–30 ng of cRNA in 30 nl of water using a solid displacement injector (Drummond Nanoject, Drummond Scientific), and measurements were carried out 2–7 days post-injection.

Macroscopic (whole-cell) current recordings were carried out under voltage clamp using an Axoclamp-2B (Axon Instruments) two-electrode clamp circuit and virtual ground. Microprocessor interface was via a μLAB/μLAN analogue/digital interface and software (WyeScience, Wye, Kent, UK). Intracellular microelectrodes were filled with 3 M KCl (input resistances, ≃1 MΩ). Connection to the amplifier headstages was via a 3 M KCl|Ag–AgCl half-cell, and matching half-cells with 3 M KCl–agar bridges were used for connection to the virtual ground. Measurements were carried out in a continuous flow of modified Ringers' solution containing 100 mM (alkali chloride plus NMG-Cl), 1 mM $MgCl_2$ and buffered with 5 mM HEPES titrated to pH 7.5 with $Ca(OH)_2$ ($[Ca^{2+}] \cong 1$ mM).

For single-channel recording, the vitelline membrane was removed manually after exposing oocytes to hypertonic 'stripping solution' (Gibb, 1995). Patch pipettes were pulled using a Narashige PP-81 puller (Narashige, Tokyo) and were fire polished. Pipettes were filled with 1 mM KCl, 99 mM NMG-Cl, 1 mM $MgCl_2$ and 5 mM Ca^{2+}-HEPES, pH 7.5, and the bath solution had an identical composition. Initial pipette resistances were 5–8 MΩ. Single-channel currents were recorded using a EPC-7 patch–clamp amplifier (List Medical, Darmstadt) after filtering at 3 kHz. Current and voltage were sampled at 44 kHz and stored on DAT tape for subsequent analysis. Offline, the data were filtered nominally at 1 kHz with a Kemo VBF4 filter (Kemo, Beckenham) and analysed using PAT v.7.0 software (Dr J.Dempster, Strathclyde Electrophysiological Software, Strathclyde). Fitting of data was carried out using a Marquardt–Levenberg algorithm (Press *et al*., 1986).

Acknowledgements

We thank Dr G.Thiel for comments on the manuscript. This work was possible with the aid of an equipment grant from the Gatsby Charitable Foundation. P.V. is supported by grant C07797 from the British Biotechnology and Biological Sciences Research Council, and D.H. is a Sainsbury PhD student.

References

Baukrowitz,T. and Yellen,G. (1995) Modulation of K^+ current by frequency and external $[K^+]$—a tale of 2 inactivation mechanisms. *Neuron*, **15**, 951–960.

Baukrowitz,T. and Yellen,G. (1996) Use-dependent blockers and exit rate of the last ion from the multiion pore of a K^+ channel. *Science*, **271**, 653–656.

Bertl,A., Slayman,C.L. and Gradmann,D. (1993) Gating and conductance in an outward-rectifying K^+ channel from the plasma membrane of *Saccharomyces cerevisiae*. *J. Membr. Biol.*, **132**, 183–199.

Blatt,M.R. (1991) Ion channel gating in plants: physiological implications and integration for stomatal function. *J. Membr. Biol.*, **124**, 95–112.

Blatt,M.R. and Gradmann,D. (1997) K^+-sensitive gating of the K^+ outward rectifier in *Vicia* guard cells. *J. Membr. Biol.*, **158**, 241–256.

Chapman,M.L., Vandongen,H.A. and Vandongen,A.J. (1997) Activation-dependent subconductance levels in the DRK1 K^+ channel suggest a subunit basis for ion permeation and gating. *Biophys. J.*, **72**, 708–719.

Choi,K.L., Aldrich,R.W. and Yellen,G. (1991) Tetraethylammonium blockade distinguishes two inactivation mechanisms in voltage-activated K^+ channels. *Proc. Natl Acad. Sci. USA*, **88**, 5092–5095.

Creighton,T.E. (1993) *Proteins*. Vol. 2. Freeman, NY.

Doyle,D.A., Cabral,J.M., Pfuetzner,R.A., Kuo,A.L., Gulbis,J.M., Cohen,S.L., Chait,B.T. and MacKinnon,R. (1998) The structure of the potassium channel: molecular basis of K^+ conduction and selectivity. *Science*, **280**, 69–77.

Gibb,A.J. (1995) Patch–clamp recording. In Ashley,R.H. (ed.), *Ion Channels: A Practical Approach*. IRL Press at Oxford University Press, Oxford, UK, pp. 1–42.

Goldbeter,A. and Koshland,D.E. (1981) An amplified sensitivity arising from covalent modification in biological systems. *Proc. Natl Acad. Sci. USA*, **78**, 6840–6844.

Goldstein,S.A.N. (1996) A structural vignette common to voltage sensors and conduction pores—canaliculi. *Neuron*, **16**, 717–722.

Groves,J.D. and Tanner,M.J.A. (1992) Glycophorin-A facilitates the expression of human band-3-mediated anion transport in *Xenopus* oocytes. *J. Biol. Chem.*, **267**, 22163–22170.

Ketchum,K.A., Joiner,W.J., Sellers,A.J., Kaczmarek,L.K. and Goldstein,S.A.N. (1995) A new family of outwardly rectifying potassium channel proteins with 2 pore domains in tandem. *Nature*, **376**, 690–695.

Kiss,L. and Korn,S.J. (1998) Modulation of C-type inactivation by K^+ at the potassium channel selectivity filter. *Biophys. J.*, **74**, 1840–1849.

Koshland,D.E., Goldbeter,A. and Stock,J.B. (1982) Amplification and adaptation in regulatory and sensory systems. *Science*, **217**, 220–225.

Lesage,F., Guillemare,E., Fink,M., Duprat,F., Lazdunski,M., Romey,G. and Barhanin,J. (1996) A pH-sensitive yeast outward rectifier K^+ channel with 2 pore domains and novel gating properties. *J. Biol. Chem.*, **271**, 4183–4187.

Liu,Y., Jurman,M.E. and Yellen,G. (1996) Dynamic rearrangement of the outer mouth of a K^+ channel during gating. *Neuron*, **16**, 859–867.

Lopez-Barneo,J., Hoshi,T., Heinemann,S.H. and Aldrich,R.W. (1993) Effects of external cations and mutations in the pore region on C-type inactivation of Shaker potassium channels. *Receptors Channels*, **1**, 61–71.

Loukin,S.H., Vaillant,B., Zhou,X.L., Spalding,E.P., Kung,C. and Saimi,Y. (1997) Random mutagenesis reveals a region important for gating of the yeast K^+ channel Ykc1. *EMBO J.*, **16**, 4817–4825.

MacKinnon,R. (1995) Pore loops—an emerging theme in ion-channel structure. *Neuron*, **14**, 889–892.

Miosga,T., Witzel,A. and Zimmermann,F.K. (1994) Sequence and function analysis of a 9.46 kb fragment of *Saccharomyces cerevisiae* chromosome X. *Yeast*, **10**, 965–973.

Ogielska,E.M., Zagotta,W.N., Hoshi,T., Heinemann,S.H., Haab,J. and Aldrich,R.W. (1995) Cooperative subunit interactions in C-type inactivation of K^+ channels. *Biophys. J.*, **69**, 2449–2457.

Pardo,L.A., Heinemann,S.H., Terlau,H., Ludewig,U., Lorra,C., Pongs,O. and Stühmer,W. (1992) Extracellular K^+ specifically modulates a rat brain K^+ channel. *Proc. Natl Acad. Sci. USA*, **89**, 2466–2470.

Press,W., Flannerly,B., Teukolsky,S. and Vetterling,W. (1986) *Numerical Recipies: The Art of Scientific Computing*. Cambridge University Press, Cambridge, UK.

Ranganathan,R., Lewis,J.H. and MacKinnon,R. (1996) Spatial localization of the K^+ channel selectivity filter by mutant cycle-based structure analysis. *Neuron*, **16**, 131–139.

Ray,F.A. and Nickoloff,J.A. (1992) Site-specific mutagenesis of almost any plasmid using a PCR-based version of unique site elimination. *Biotechniques*, **13**, 342–344.

Reid,J.D., Lukas,W., Shafaatian,R., Bertl,A., Scheurmannkettner,C., Guy,H.R. and North,R.A. (1996) The *Saccharomyces cerevisiae* outwardly-rectifying potassium channel (DUK1) identifies a new family of channels with duplicated pore domains. *Receptors Channels*, **4**, 51–62.

Richard,E.A. and Miller,C. (1990) Steady-state coupling of ion-channel conformations to a transmembrane ion gradient. *Science*, **247**, 1208–1210.

Schlief,T., Schonherr,R. and Heinemann,S.H. (1996) Modification of C-type inactivating shaker potassium channels by chloramine-T. *Pflugers Arch.*, **431**, 483–493.

Schneggenburger,R. and Ascher,P. (1997) Coupling of permeation and gating in an NMDA-channel pore mutant. *Neuron*, **18**, 167–177.

Sun,Z.P., Akabas,M.H., Goulding,E.H., Karlin,A. and Siegelbaum,S.A. (1996) Exposure of residues in the cyclic nucleotide-gated channel pore—P-region structure and function in gating. *Neuron*, **16**, 141–149.

Thiel,G. and Wolf,A.H. (1997) Operation of K^+ channels in stomatal movement. *Trends Plant Sci.*, **2**, 339–345.

Vergani,P., Miosga,T., Jarvis,S.M. and Blatt,M.R. (1997) Extracellular K^+ and Ba^{2+} mediate voltage-dependent inactivation of the outward-rectifying K^+ channel encoded by the yeast gene *TOK1*. *FEBS Lett.*, **405**, 337–344.

Wang,S.M., Morales,M.J., Liu,S.G., Strauss,H.C. and Rasmussen,R.L. (1997) Modulation of HERG affinity for E-4031 by $[K^+]_o$ and C-type inactivation. *FEBS Lett.*, **417**, 43–47.

Yellen,G., Sodickson,D., Chen.T.-Y. and Jurman,M.E. (1994) An engineered cysteine in the external mouth of a K^+ channel allows inactivation to be modulated by metal binding. *Biophys. J.*, **66**, 1068–1075.

Zhou,X.L., Vaillant,B., Loukin,S.H., Kung,C. and Saimi,Y. (1995) Ykc1 encodes the depolarization-activated K^+ channel in the plasma membrane of yeast. *FEBS Lett.*, **373**, 170–176.

Received July 7, 1998; revised October 5, 1998; accepted October 15, 1998